

Mass spectrometric study of aged benzene secondary organic aerosol in the presence of dry ammonium sulfate

Mingqiang Huang^{1,2,3} · Jiahui Zhang¹ · Shunyou Cai^{1,2} ·
Yingmin Liao³ · Weixiong Zhao⁴ · Changjin Hu⁴ ·
Xuejun Gu⁴ · Li Fang⁴ · Weijun Zhang⁴

Received: 23 June 2015 / Accepted: 27 January 2016 /
Published online: 2 February 2016
© Springer Science+Business Media Dordrecht 2016

Abstract Inorganic seed particles have relatively large surface area, and play an important role in the formation and aging of secondary organic aerosol (SOA). The effects of dry $(\text{NH}_4)_2\text{SO}_4$ which is the most commonly found in urban atmosphere on the aged benzene SOA were qualitatively studied utilizing aerosol laser time-of-flight mass spectrometer (ALTOFMS) coupled with Fuzzy C-Means (FCM) clustering algorithm in this study. Experimental results indicated that nitrophenol, oxocarboxylic acid, epoxide products are the predominant components in the aged benzene SOA in the presence of low concentration (about $10 \mu\text{g m}^{-3}$) of dry $(\text{NH}_4)_2\text{SO}_4$. These aged products are the same as the previously obtained aged benzene SOA without $(\text{NH}_4)_2\text{SO}_4$ seed aerosol, indicating that low concentration of dry $(\text{NH}_4)_2\text{SO}_4$ acts just as the nucleation or condensation center of the SOA, and do not affect the chemical composition of SOA. However, 1 H-imidazole, 1 H-imidazole-2-carbaldehyde, hydrated 1 H-imidazole-2-carbaldehyde, 2,2'-biimidazole, hydrated N-glyoxal substituted 1 H-imidazole, N-glyoxal substituted hydrated 1 H-imidazole-2-carbaldehyde, mono glyoxal substituted hydrated 1 H-imidazole-2-carboxaldehyde, mono glyoxal substituted 2,2'-biimidazole and hydrated glyoxal dimer substituted imidazole which are formed from ammonium ion reaction with glyoxal are the major particulate products in the aged benzene SOA in the presence of high concentration

Electronic supplementary material The online version of this article (doi:10.1007/s10874-016-9328-6) contains supplementary material, which is available to authorized users.

✉ Weijun Zhang
wjzhang@aiofm.ac.cn

¹ College of Chemistry & Environment, Minnan Normal University, Zhangzhou 363000, China

² Fujian Province Key Laboratory of Modern Analytical Science and Separation Technology, Zhangzhou 363000, China

³ Department of Environmental Science and Engineering, Tan Kah Kee College, Xiamen University, Zhangzhou 363105, China

⁴ Laboratory of Atmospheric Physico-Chemistry, Anhui Institute of Optics and Fine Mechanics, Chinese Academy of Sciences, Hefei 230031, China

(about $100 \mu\text{g m}^{-3}$) of dry $(\text{NH}_4)_2\text{SO}_4$. The retention of water on the dry $(\text{NH}_4)_2\text{SO}_4$ particles creates ammonium ion, which can promote the formation of high-molecular-weight (HMW) products through multiphase reactions such as hydration and polymerization of aldehydes from OH-initiated oxidation of benzene.

Keywords Benzene · Secondary organic aerosol · Ammonium sulfate · Seed aerosol · Laser desorption/ionization · Aging mechanism

1 Introduction

Secondary organic aerosol (SOA) particles formed from photooxidation of aromatic hydrocarbons emitted from motor vehicles can undergo continuous physical and chemical processing, commonly called aging (Robinson et al. 2007; Rudich et al. 2007; Andreae 2009; Pillar et al. 2014). Aging processes comprise oxidation reactions of semivolatile precursors in the gas phase, multiphase reactions (Robinson et al. 2007; Rudich et al. 2007; Andreae 2009), and reactions at multiphase interfaces, e.g., aging of polyphenols in aromatic SOA can continue mediated by a mechanism of ozonolysis at air–water interfaces. This pathway can contribute precursors to aqueous SOA formation, converting aromatic hydrocarbons into polyfunctional species widely found in tropospheric aerosols (Pillar et al. 2014). The aged SOA particles have greater hygroscopicity, toxicity, and optical absorption ability (Ng et al. 2011; Tritscher et al. 2011; Sareen et al. 2013), and are believed to affect climate (Lee et al. 2014), visibility (Baltensperger 2010; Singh and Dey 2012) and human health (Topinka et al. 2011; Sorooshian et al. 2012). The aging process of aromatic SOA is currently a focus of research interest in the field of atmospheric chemistry. Loza et al. (2012) have presented the formation and aging of SOA from the photooxidation of *m*-xylene under low- NO_x conditions (below 2 ppb detection of the instrument) and in the presence of either neutral or acidic ammonium sulfate seed particles in laboratory chambers, and observed the O/C ratio of the aged products increased continuously starting after 5 h of irradiation until the 36 h termination. Sato et al. (2012) and Huang et al. (2014) have identified the nitrophenol, oxocarboxylic acids and epoxide products of the aged benzene SOA with liquid chromatography/time-of-flight mass spectrometry (LC/MS) and aerosol laser time-of-flight mass spectrometer (ALTOFMS), respectively. Recently, The effects of NH_3 and NO_x on the optical properties of aromatic aged SOA were investigated by Updyke et al. (2012) and Nakayama et al. (2013) using UV-Vis absorption spectra and cavity ring-down spectroscopy (CRDS), respectively, and the light-absorbing ability of the aged SOA was found to enhance with increasing initial NH_3 and NO_x concentrations.

As is known to all, there are a variety of fine inorganic aerosol particles in the atmosphere. These particles have relatively large surface area, can be used as seed aerosol (Jang et al. 2002; Wang et al. 2011). However, most of these aging studies mention above were performed without or with relatively low concentrations of inorganic seed aerosols. Ammonium sulfate ($(\text{NH}_4)_2\text{SO}_4$), which formed by the reaction of ammonia with sulphuric acid is one of the most common inorganic seed aerosols in the atmosphere (Robinson et al. 2013). Previous smog chamber studies were focused on the effect of dry $(\text{NH}_4)_2\text{SO}_4$ seed aerosol on the aromatic SOA yield. Cocker et al. (2001) found that low mass concentration (about $0.2 \sim 40 \mu\text{g m}^{-3}$) of dry $(\text{NH}_4)_2\text{SO}_4$ seed aerosol had no significant effect on aromatic SOA formation. In contrast, Lu et al. (2009), who have shown that SOA formation from photooxidation of *m*-xylene was enhanced in the presence of high mass concentration (about $40 \sim 100 \mu\text{g m}^{-3}$) of dry $(\text{NH}_4)_2\text{SO}_4$

seed aerosol. Their result implies that the dry $(\text{NH}_4)_2\text{SO}_4$ seed aerosol has no (or nondetectable) effect on SOA formation when its concentration is lower than a threshold (this threshold is between 7 and 11 $\text{cm}^2 \text{m}^{-3}$), whereas the SOA yield increases above a concentration threshold. Recently, Chhabra et al. (2010); Qi et al. (2010) and Loza et al. (2012) have measured the aged *m*-xylene SOA in the presence of dry $(\text{NH}_4)_2\text{SO}_4$ seed aerosol using an aerodyne high-resolution aerosol mass spectrometer, and observed the O/C ratio of the aged products increased corresponding to volatility decreased and hydrophilicity increased. Nevertheless, the detail chemical compositions of the aged aromatic SOA were not reported in these aging studies. Also, previous aging studies were conducted with low concentrations of dry $(\text{NH}_4)_2\text{SO}_4$ seed aerosol, no investigations on the effects on the chemical composition of the aged aromatic SOA in the presence of high mass concentration of $(\text{NH}_4)_2\text{SO}_4$ seed aerosol are performed up to now.

With the rapid development of China's economy, the extensive use of coal and oil, makes urban atmosphere contains a high concentration of SO_2 (Schreier et al. 2015). Meanwhile, China is a large agricultural country, agricultural production and livestock breeding industry emit lots of ammonia per year, resulting in high concentration of ammonium sulfate in urban atmosphere (Tong and Xu 2012). For example, the annual average concentration of aerosol particles in Beijing is about $100 \mu\text{g m}^{-3}$, and during haze days it may exceed $300 \mu\text{g m}^{-3}$, one-third of which are inorganic ionic species (mainly SO_4^{2-} , NO_3^- and NH_4^+) (He et al. 2001; Wang et al. 2006). Our group has used scanning mobility particle sizer and ALTOFMS to study the effects of inorganic seed aerosols on the growth and chemical composition of SOA formed from OH-initiated oxidation of toluene. Our results revealed that inorganic seed aerosols would promote growth rates of SOA formation at the start of the reaction and inhibits its formation rate with prolonging the reaction time, while the products of SOA is affected by inorganic seed aerosol through multiphase reaction (Huang et al. 2013a). Recently, Fuzzy C-Means (FCM) algorithm has been developed by our group to classify the mass spectra of large numbers of particles obtained by ALTOFMS (Huang et al. 2013b). And the latest study demonstrate that FCM allowed a clear identification of eleven distinct chemical particle classes in the aged benzene SOA, showing that the real-time ALTOFMS detection approach coupled with the FCM data processing algorithm can make cluster analysis of SOA successfully (Huang et al. 2014). Based on this, the effects of low (about $10 \mu\text{g m}^{-3}$) and high (about $100 \mu\text{g m}^{-3}$) mass concentrations of dry $(\text{NH}_4)_2\text{SO}_4$ seed aerosol on the aged benzene SOA were qualitatively studied using ALTOFMS coupled with FCM algorithm in this study. The chemical composition of the aged benzene SOA in the presence of dry $(\text{NH}_4)_2\text{SO}_4$ seed aerosol were obtained, and the possible reaction mechanisms leading to these aged products were also discussed.

2 Experimental

2.1 Material

Benzene (>99 %) was bought from Sigma-Aldrich Chemistry Corporation, Germany. Sodium nitrite (> 99 %), methanol (> 99 %) and ammonium sulfate (> 99 %) were obtained from The Third Reagent Factory of Tianjin. Nitric oxide (99.9 %) was provided by Nanjing Special Gas Factory. Methyl nitrite was prepared and purified by the method provided in our previous studies (Huang et al. 2013a; Huang et al. 2014; Huang et al. 2015), and preserved in liquid nitrogen until use.

2.2 Generation of dry $(\text{NH}_4)_2\text{SO}_4$ seed aerosols

As shown in Fig. 1, dry $(\text{NH}_4)_2\text{SO}_4$ seed aerosol was generated by aspirating 0.001 mol/L salt solution (0.066 g $(\text{NH}_4)_2\text{SO}_4$ dissolved in 500 mL deionized water) through a constant output atomizer (TSI Inc. Model 3076), and subsequently passed through a diffusion dryer (TSI Inc. Model 3062) (with exiting RH lower than 20 %), an ^{85}Kr charge neutralizer (TSI Inc., Model 3077) (excluding charges into neutral aerosol) before entering smog chamber. The generated dry $(\text{NH}_4)_2\text{SO}_4$ seed aerosol was 10,000–50,000 particles cm^{-3} with mean diameter of about 100 nm, and the concentration of the $(\text{NH}_4)_2\text{SO}_4$ seed aerosol in the smog chamber is about 10 or 100 $\mu\text{g m}^{-3}$ by controlling the flow rate of zero air.

2.3 Benzene SOA aging in the presence of dry $(\text{NH}_4)_2\text{SO}_4$ seed aerosol

The formation and aging benzene SOA were performed using UV-irradiation of benzene/ CH_3ONO /NO/air mixtures in a smog chamber, the overall system components have been presented in detail previously (Huang et al. 2014; Huang et al. 2015). In all experiments, the temperature and relative humidity (RH) in the smog chamber were measured continuously by temperature and humidity sensor (Vaisala HMT333, Finland). The temperature and relative humidity in chamber was maintained at about 25 ± 4 °C and 15 ± 2 %, respectively. After flushing the smog chamber and obtaining the desired dry $(\text{NH}_4)_2\text{SO}_4$ seed aerosol, benzene was sampled by a micro liter injector and delivered to the chamber by sending air through a small heated glass tube. NO and CH_3ONO were expanded into the evacuated manifold to the desired pressure through Teflon lines, and introduced into the smog chamber, mixed with the pre-existing purified air and dry $(\text{NH}_4)_2\text{SO}_4$ seed aerosol. The chamber was filled with the purified air to 850 L full volume. The concentrations of benzene and methyl nitrate were monitored by GC-FID (Agilent 7820 A, USA) and ultraviolet–visible spectroscopy of Chermis cell system, respectively. Nitric oxide and nitrogen dioxide were measured by NO-NO₂-NO_x analyzer (TEI model 42i). The mass concentration and mean diameter of seed aerosols were measured by scanning mobility particle sizer (SMPS; TSI 3080 L DMA, TSI 3775 CPC). The concentration of benzene, CH_3ONO , NO and $(\text{NH}_4)_2\text{SO}_4$ seed aerosol is 2.0 ppm, 20.0 ppm, 2.0 ppm, and about 10 (or 100) $\mu\text{g m}^{-3}$, respectively. Then, 4 black lamps were turned on and the photooxidation reaction was initiated. OH radicals are generated by the irradiation of methyl nitrite with black lamps whose wavelength in range of 300–400 nm (Atkinson et al. 1981). In each experiment, the OH concentration reached a maximum immediately after turning on black lamps and then decreased with time, but the OH concentration maintained $>0.5 \times 10^6$ molecules cm^{-3} during irradiation, which is slightly less than the average global atmospheric concentration

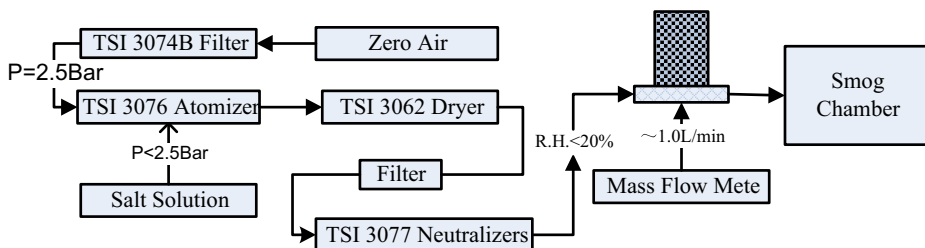


Fig. 1 Schematic of the $(\text{NH}_4)_2\text{SO}_4$ seed aerosol generating system

of OH radicals of about 10^6 molecules cm^{-3} (Prinn et al. 2001). This indicates that particles and vapors in the reaction chamber were continuously oxidized during irradiation (Huang et al. 2014; Huang et al. 2015). After 24 h photooxidation, the aged benzene SOA particles are analyzed continuously using the ALTOFMS connected directly to the chamber using a Teflon line. The obtained aged particles were Fuzzy c-means algorithm (FCM) (Bezdek 1981) clustered based on their individual mass spectrum as described in detail in our previous studies (Huang et al. 2013b; Huang et al. 2014; Huang et al. 2015).

3 Results and discussion

The time series of the benzene and SOA mass concentrations (raw and corrected for wall-loss correction) measured are shown in Fig. 2. A density of 1.23 g/cm^3 , calculated by comparing the electronic mobility diameter from the SMPS and vacuum aerodynamic diameter from ALFOFMS, was employed to estimate SOA mass concentrations (Huang et al. 2013a). For the seeded experiments, SOA mass concentrations were obtained by subtracting the initial seed aerosol mass concentrations. SOA mass is corrected for wall loss assuming a first-order loss rate calculated by fitting the particle number concentration decay at the end of each experiment (Huang et al. 2013a). As shown in Fig. 2, less than 30 min after turning on blank lamps, a monomodal SOA formation could be detected using a SMPS measurement. This aerosol grew in number of particles and mass for the first 30 min and then reached a maximum at 6 h, where no benzene was left in the chamber according to GC data. Before 6 h in our study, there were plenty of benzene and OH radicals to generate much more SOA particles than they were lost,

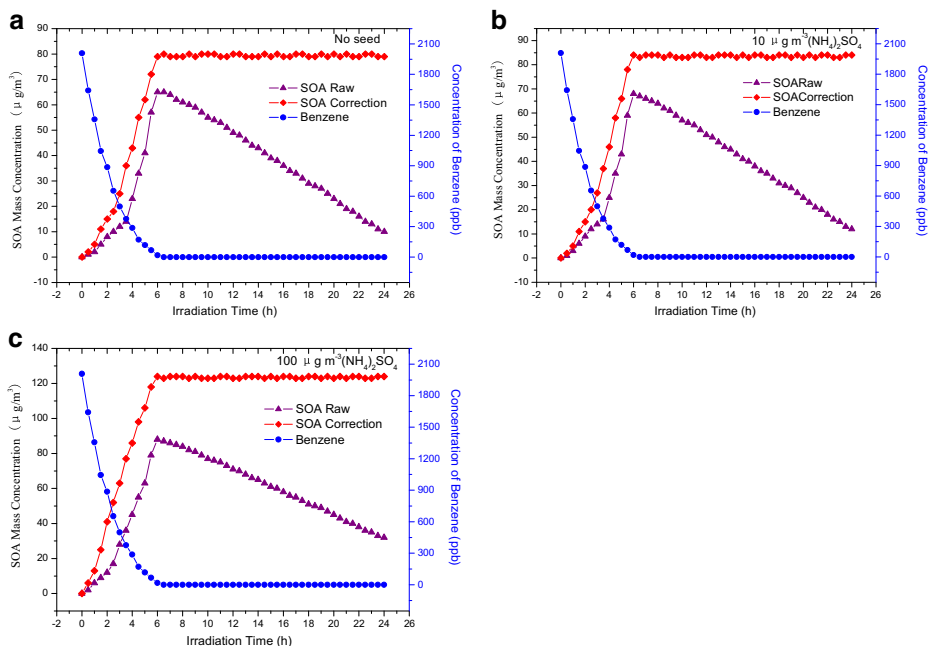


Fig. 2 The benzene and SOA mass concentrations (raw and corrected for wall-loss correction) measured as a function of irradiation time in the presence of (a) no seed, (b) $10 \mu\text{g m}^{-3} (\text{NH}_4)_2\text{SO}_4$ and (c) $100 \mu\text{g m}^{-3} (\text{NH}_4)_2\text{SO}_4$

where we observed the mass increase. While afterwards, there was not benzene available in smog chamber, SOA aging processes occur, and the aged benzene SOA particles deposited onto the chamber wall due to turbulence, Brownian diffusion and gravitational sedimentation of particles (Bowman et al. 1997), causing the aerosol losses. The SOA mass concentration profile in the presence of $10 \mu\text{g m}^{-3}$ of dry $(\text{NH}_4)_2\text{SO}_4$ seed aerosol is very similar to that the unseeded experiment (the corrected maximum mass concentration of SOA is $80 \mu\text{g m}^{-3}$ for these two experiments) indicating that low concentration of dry $(\text{NH}_4)_2\text{SO}_4$ seed aerosol does not change the gas/particle partitioning and SOA formation. However, the presence of $100 \mu\text{g m}^{-3}$ of dry $(\text{NH}_4)_2\text{SO}_4$ seed aerosol increases the mass concentration of SOA. According to Fig. 2(c), the corrected maximum mass concentration of SOA in the presence of high concentration of dry $(\text{NH}_4)_2\text{SO}_4$ seed aerosol is $120 \mu\text{g m}^{-3}$, higher than those observed for the unseeded or low concentration seed aerosol experiments. The effects on the chemical composition of the aged benzene SOA in the presence of dry $(\text{NH}_4)_2\text{SO}_4$ seed aerosol are discussed in the following sections.

3.1 The influence of low concentration of dry $(\text{NH}_4)_2\text{SO}_4$ on the aged benzene SOA

As shown in our previous studies (Huang et al. 2007; Huang et al. 2013b; Huang et al. 2014), the particle's mass spectrum is only acquired from the one whose diameter has been measured by ALTOFMS. 5 812 single particle mass spectra of the aged benzene SOA particles were obtained in the presence of low mass concentration (about $10 \mu\text{g m}^{-3}$) of $(\text{NH}_4)_2\text{SO}_4$ seed aerosol. After setting the FCM initial clustering number (n) from 2 to 30, fuzzy degrees parameter (m) to 2, the biggest cycles for 500, and the precision of the clustering to 0.1, the Davies-Bouldin index displayed in Fig. 3(a) has the minimum value at $n = 12$, suggesting these aged SOA particles can be clustered into 12 classes. Figure 4 exhibits the determined spectra patterns as the cluster centers of these twelve classes. The spectra patterns are displayed in analogy to real time-of-flight mass spectra of aromatic SOA particles obtained in our previous study (Huang et al. 2007; Huang et al. 2013b) as positive ion “signals”, with the signal intensities representing the vector components of the cluster center.

The mass spectrum of class 1 contains the only peak of m/z 18 (NH_4^+), corresponding to the $(\text{NH}_4)_2\text{SO}_4$ particles (Huang et al. 2013a). The spectra patterns of the second to 12th class

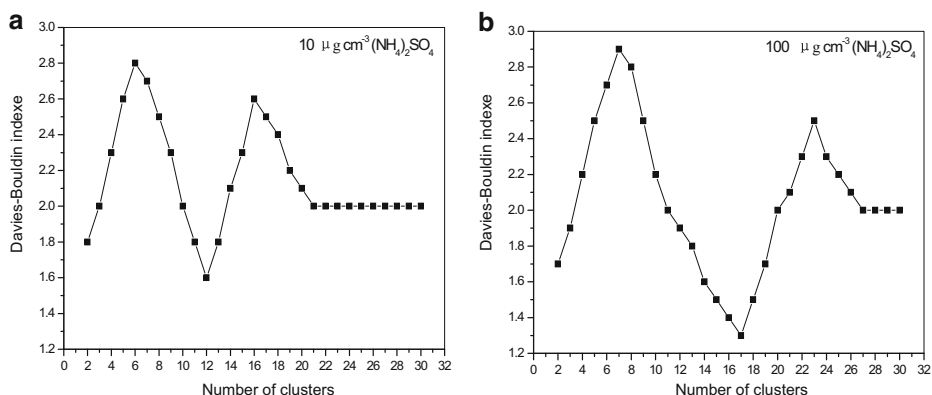


Fig. 3 The clustering number was evaluated using Daviese-Bouldin index for the aged benzene SOA particles in the presence of (a) $10 \mu\text{g m}^{-3}$ $(\text{NH}_4)_2\text{SO}_4$ and (b) $100 \mu\text{g m}^{-3}$ $(\text{NH}_4)_2\text{SO}_4$

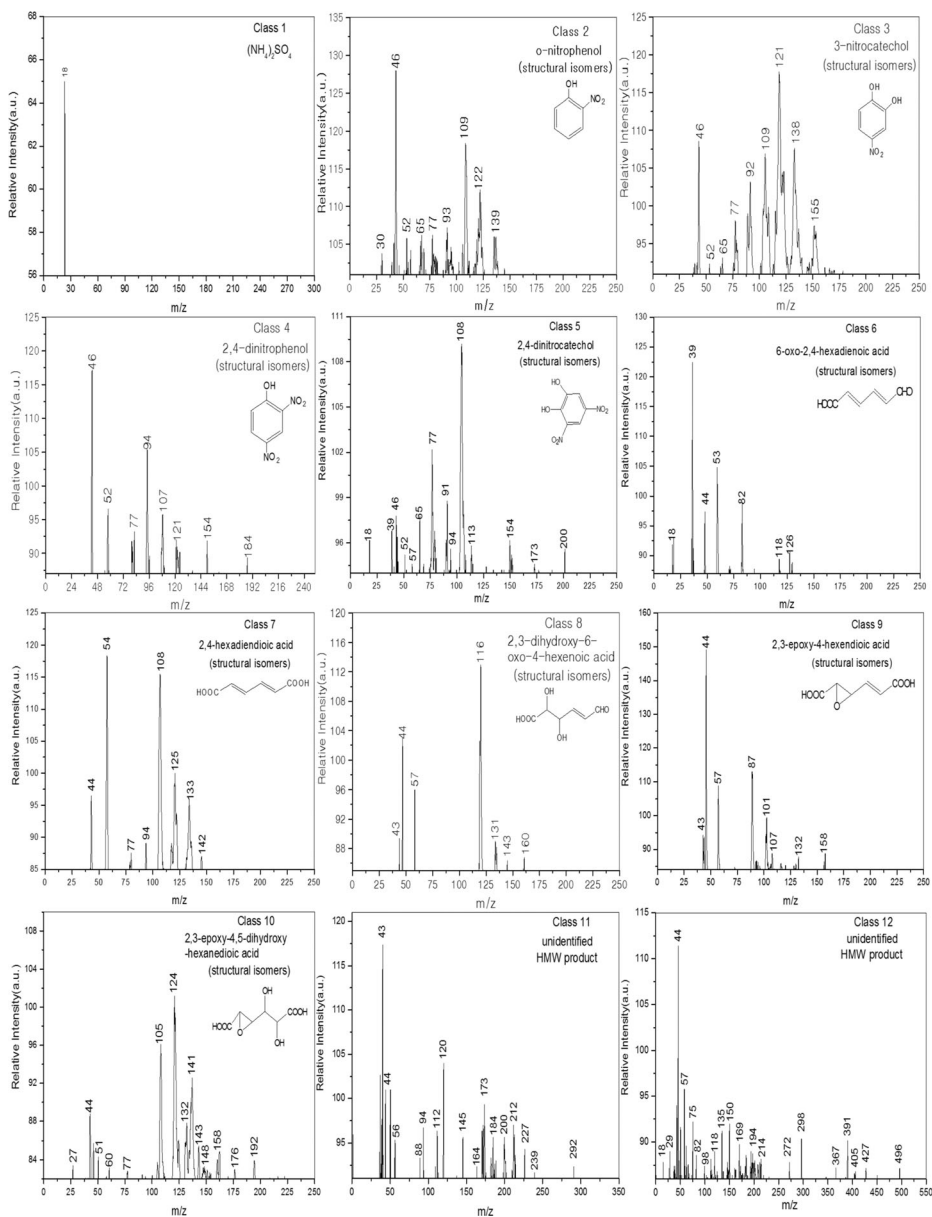
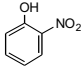
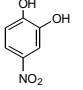
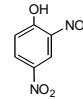
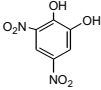
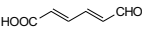
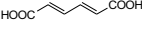
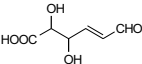
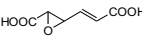
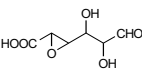


Fig. 4 Representative spectra patterns of the aged benzene SOA particles in the presence of $10 \mu\text{g m}^{-3}$ dry $(\text{NH}_4)_2\text{SO}_4$ determined by FCM

were consistent with the mass spectra of the aged products measured in our previous benzene SOA aged experiment without $(\text{NH}_4)_2\text{SO}_4$ seed aerosol (Huang et al. 2014). The molecular ion peak, possible cleavage fragment peaks and speculated molecular structure of the aged products were listed in Table 1. It can be seen from the Table 1 that nitrophenol, dinitrophenol, nitrocatechol, dinitrocatechol, 6-oxo-2,4-hexadienoic acid, 2,4-hexadiendioic acid, 2,3-dihydroxy-6-oxo-4-hexenoic acid, 2,3-epoxy-4-hexendioic acid, 2,3-epoxy-4,5-dihydroxy-hexanedioic acid

Table 1 Molecular structure of the speculated particulate products of the aged benzene SOA in the presence of low concentration of dry $(\text{NH}_4)_2\text{SO}_4$ seed aerosol

Cluster Number	Observed M^+ ion	Possible fragment ions (m/z)	Speculated structure	Ref. & comment
2	139	122($\text{C}_6\text{H}_3\text{NO}_2^+$); 109($\text{C}_6\text{H}_5\text{O}_2^+$); 93($\text{C}_6\text{H}_5\text{O}^+$); 77 (C_6H_5^+); 65 (C_5H_5^+); 52 (C_4H_4^+); 46 (NO_2^+)		Sato et al.(2012) Huang et al.(2014)
3	155	138 ($\text{C}_6\text{H}_4\text{NO}_3^+$); 122($\text{C}_6\text{H}_3\text{NO}_2^+$); 109 ($\text{C}_6\text{H}_5\text{O}_2^+$); 92 ($\text{C}_6\text{H}_4\text{O}^+$); 77 (C_6H_5^+); 65 (C_5H_5^+); 52 (C_4H_4^+); 46 (NO_2^+)		Sato et al.(2012) Huang et al.(2014)
4	184	154 ($\text{C}_6\text{H}_4\text{NO}_4^+$); 121 ($\text{C}_6\text{H}_3\text{NO}_2^+$); 107 ($\text{C}_6\text{H}_5\text{O}_2^+$); 92 ($\text{C}_6\text{H}_4\text{O}^+$); 77 (C_6H_5^+); 52 (C_4H_4^+); 46 (NO_2^+);		Sato et al.(2012) Huang et al.(2014)
5	200	154 ($\text{C}_6\text{H}_4\text{NO}_4^+$); 108 ($\text{C}_6\text{H}_4\text{O}_2^+$); 91($\text{C}_6\text{H}_3\text{O}^+$) 77 (C_6H_5^+); 65 (C_5H_5^+); 52 (C_4H_4^+); 46 (NO_2^+); 39 (C_3H_3^+); 18 (H_2O^+)		Sato et al.(2012) Huang et al.(2014)
6	126	82 ($\text{C}_5\text{H}_6\text{O}^+$); 53 (C_4H_5^+); 44 (CO_2^+); 39 (C_3H_3^+); 18 (H_2O^+)		Sato et al.(2012) Huang et al.(2014)
7	142	125 ($\text{C}_6\text{H}_5\text{O}_3^+$); 108 ($\text{C}_6\text{H}_4\text{O}_2^+$); 54 (C_4H_6^+); 44 (CO_2^+)		Sato et al.(2012) Huang et al.(2014)
8	160	143($\text{C}_6\text{O}_4\text{H}_7^+$); 131($\text{C}_5\text{O}_4\text{H}_7^+$); 116($\text{C}_4\text{O}_4\text{H}_4^+$); 44(CO_2^+)		Sato et al.(2012) Huang et al.(2014)
9	158	101 ($\text{C}_4\text{H}_4\text{O}_3^+$); 87 ($\text{C}_3\text{H}_3\text{O}_3^+$); 57 (C_2HO_2^+); 44 (CO_2^+)		Sato et al.(2012) Huang et al.(2014)
10	192	158 ($\text{C}_6\text{H}_6\text{O}_5^+$); 148($\text{C}_5\text{H}_8\text{O}_5^+$); 141($\text{C}_6\text{H}_5\text{O}_4^+$); 124 ($\text{C}_6\text{H}_4\text{O}_3^+$); 105 ($\text{C}_3\text{H}_3\text{O}_4^+$); 44 (CO_2^+)		Sato et al.(2012) Huang et al.(2014)

and high-molecular-weight (HMW) components were also the predominant products in the aged benzene SOA particles. Phenol, 6-oxo-2,4-hexadienal, and 2,3-epoxy- 6-oxo-4-hexenal are observed to be the major products formed from OH-initiated oxidation of benzene (Martín-Reviejo and Wirtz 2005; Borrás and Tortajada-Genarob 2012; Wang et al. 2013). These products could condense on the existing $(\text{NH}_4)_2\text{SO}_4$ seed aerosol to form SOA. As shown by Sato et al. (2012) and Huang et al. (2014), benzene SOA aging proceeds through the oxidation of the internal double bond of ring-opened products and oxocarboxylic acids and epoxide products formation resulting from the OH-initiated oxidation of the carbonyl group. Organic nitrogen-containing products formation from phenol is initiated by reactions with OH radicals, and react with NO_2 subsequently. These results are consistent with the findings of Cocker et al. (2001) and Lu et al. (2009), suggesting that low concentration of dry $(\text{NH}_4)_2\text{SO}_4$ acts just as the nucleation or condensation center of the SOA, and do not affect the chemical composition of SOA.

3.2 The influence of high concentration of dry $(\text{NH}_4)_2\text{SO}_4$ on the aged benzene SOA

6 145 single particle mass spectra of the aged benzene SOA particles were obtained in the presence of high mass concentration (about $100 \mu\text{g m}^{-3}$) of dry $(\text{NH}_4)_2\text{SO}_4$ seed aerosol, and 17 classes displayed in Fig. 3(b) were obtained by FCM clustering analysis as described above. From Fig. 5 it can be seen that the mass spectrum of these 17 clusters is different from that of our previously obtained aged benzene SOA in the presence of low mass concentration of dry $(\text{NH}_4)_2\text{SO}_4$ seed aerosol, indicating that new aged products are formed. The first class was attributed to $(\text{NH}_4)_2\text{SO}_4$ particles, as its mass spectrum contains the only peak of m/z 18 (NH_4^+) (Huang et al. 2013a). The spectra patterns of the second and third class were consistent with the mass spectra of glyoxal and 6-oxo-2,4-hexadienal which were measured in our previous photooxidation experiment of aromatic compounds (Huang et al. 2007; Huang et al. 2013b), suggesting these two compounds existed in the aged benzene SOA particles. The mass spectrum of 4th to 12th class have characteristic cleavage fragment peaks m/z 41 ($\text{C}_2\text{H}_3\text{N}^+$) and m/z 67 ($\text{C}_3\text{H}_3\text{N}_2^+$), indicating that these clusters belong to the imidazole compound (Yu et al. 2011; Kampf et al. 2012). Table 2 lists the molecular ion peak, possible cleavage fragment peaks and speculated molecular structure of imidazole products.

The clustering results show that high mass concentration of dry $(\text{NH}_4)_2\text{SO}_4$ seed aerosol can promote the formation of imidazole compounds in the aged benzene SOA. According to experimental results of Meyer et al. (2008), dry $(\text{NH}_4)_2\text{SO}_4$ seed aerosol can form ammonium ion (NH_4^+) by absorbing water. Ammonium ion is a weak acid with dissociation constant K_a of 5.6×10^{-10} ($\text{p}K_a = 9.25$), it is very difficult to be hydrolyzed to generate hydronium ($\text{NH}_4^+ + \text{H}_2\text{O} \rightarrow \text{NH}_3 + \text{H}_3\text{O}^+$). In fact, any hydronium available through this equilibrium should actually come from H_2SO_4 or H_2SO_4 (Rincón et al. 2009; Rincón et al. 2010). However, ammonium ion was found to react with α -dicarbonyl compounds, such as glyoxal and methyl glyoxal to form imidazole products in previous experiments (Nozière et al. 2009; Yu et al. 2011; Kampf et al. 2012). Smog chamber studies have indicated that glyoxal is the major aldehyde products formed from OH-initiated oxidation of benzene (Martín-Reviejo and Wirtz 2005; Borrás and Tortajada-Genarob 2012; Wang et al. 2013), the generated glyoxal could condense on the existing dry $(\text{NH}_4)_2\text{SO}_4$ seed aerosol. As shown in Fig. 6, ammonium ion acts as in two ways: by acting as a Bronsted acid (i.e., releasing protons) or forming covalent nitrogen species such as iminium intermediates (Nozière et al. 2009; Yu et al. 2011; Kampf et al. 2012). Accordingly, in the latter pathway of this mechanism, glyoxal is protonated by the ammonium ion, and the protonated glyoxal can undergo nucleophilic attack by ammonia followed by loss of water and H^+ ion, giving the diimine (1). In the other pathway, glyoxal is protonated by the ammonium ion and subsequently be hydrolyzed by diol product (2) and tetrol product (3) formation, respectively, as in the classical acid-catalyzed mechanism (Nozière et al. 2009; Yu et al. 2011; Kampf et al. 2012).

Diimine (1) reacts with tetrol product (3) to produce (4) via the dehydration reaction of hydrogen atom of amido of (1) and the OH of (3). (4) is unstable, the lone pair electrons of N atom could nucleophilic attack the C atom, leading to the formation of (5) after dehydration. (5) produces formic acid and 1 H-imidazole (I) (6) through electronic rearrangement and fracture dehydration reaction (Yu et al. 2011; Kampf et al. 2012). The formed (6) can continue to react with (3) to generate hydrated N-glyoxal substituted 1 H-imidazole (HGI) (7) and hydrated glyoxal dimer substituted imidazole (HGGI) (8) after dehydration, respectively (Yu et al. 2011; Kampf et al. 2012). In addition, (5) can also occur electron rearrangement shown in Fig. 6 to form the hydrated 1 H-imidazole-2-carbaldehyde (HIC) (9). (9) can be dehydrated to

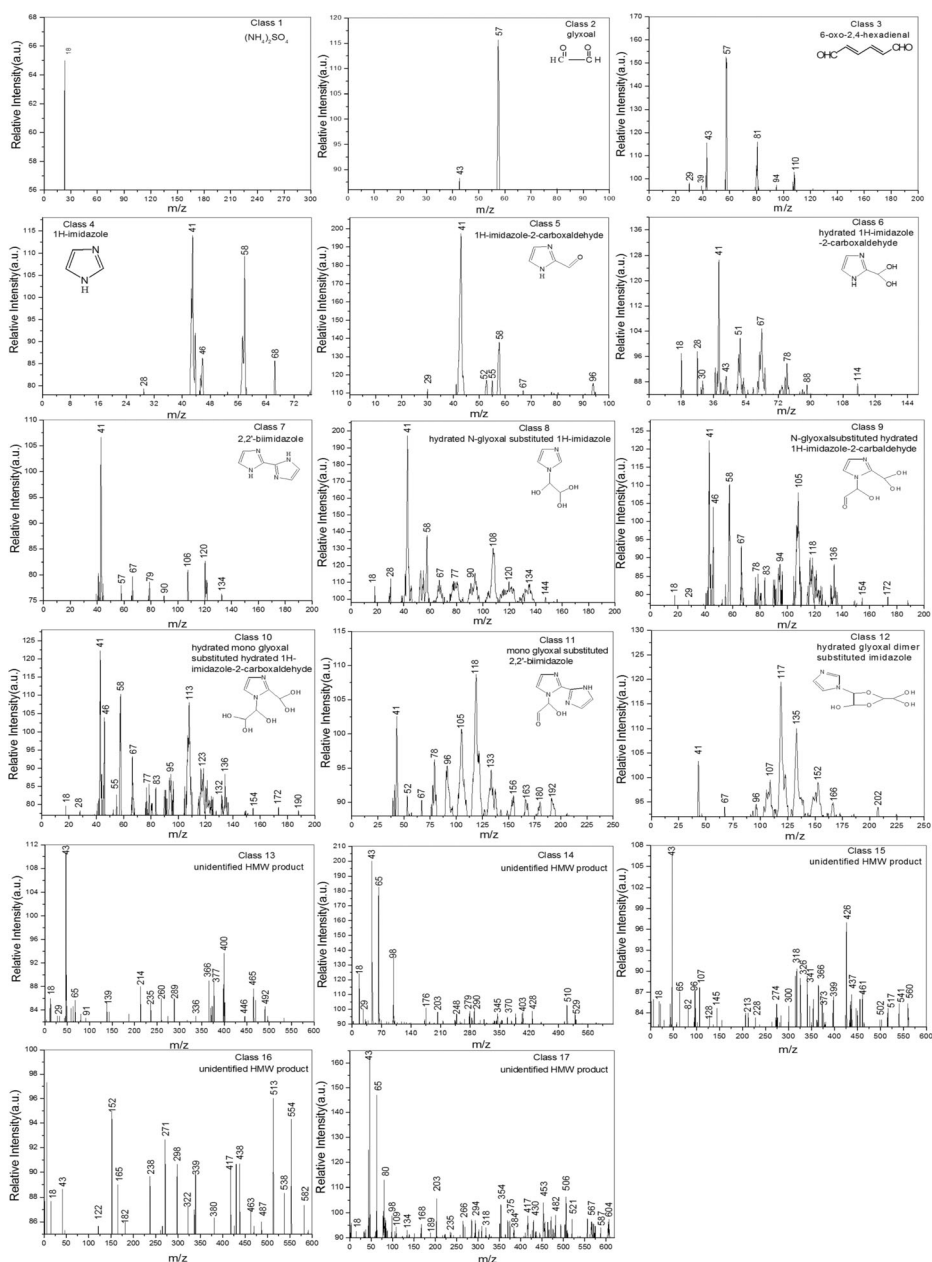


Fig. 5 Representative spectra patterns of the aged benzene SOA particles in the presence of $100 \mu\text{g m}^{-3}$ dry $(\text{NH}_4)_2\text{SO}_4$ determined by FCM

generate 1 H-imidazole-2-carbaldehyde (IC) (10), or continue to react with (2) to form N-glyoxal substituted hydrated 1 H-imidazole-2-carboxaldehyde (GHIC) (11) after dehydration, (11) further hydration to get hydrated mono glyoxal substituted hydrated 1 H-imidazole-2-carboxaldehyde (HGHIC) (12) (Yu et al. 2011; Kampf et al. 2012). According to the theory of Kampf et al. (2012), hydrated 1 H-imidazole-2-carboxaldehyde (9) can also react with (5) to form

Table 2 Molecular structure of the speculated particulate products of the aged benzene SOA in the presence of high concentration of dry $(\text{NH}_4)_2\text{SO}_4$ seed aerosol

Cluster Number	Observed M^+ ion	Possible fragment ions (m/z)	Speculated structure	Ref. & comment
2	57	57(HCOCO^+)		Huang et al.(2013b)
3	110	81 ($\text{C}_3\text{H}_5\text{O}^+$); 29 (HCO^+)		Huang et al.(2007) Huang et al.(2013b)
4	68	41($\text{C}_2\text{H}_3\text{N}^+$); 28(CH_2N^+)		Yu et al.(2011) Kampf et al.(2012)
5	96	67($\text{C}_3\text{H}_3\text{N}_2^+$); 41($\text{C}_2\text{H}_3\text{N}^+$); 29 (HCO^+)		Yu et al.(2011) Kampf et al.(2012)
6	114	78 ($\text{C}_4\text{H}_2\text{N}_2^+$); 67($\text{C}_3\text{H}_3\text{N}_2^+$); 41($\text{C}_2\text{H}_3\text{N}^+$); 28(CH_2N^+); 18(H_2O^+)		Yu et al.(2011) Kampf et al.(2012)
7	134	67($\text{C}_3\text{H}_3\text{N}_2^+$); 41($\text{C}_2\text{H}_3\text{N}^+$)		Yu et al.(2011) Kampf et al.(2012)
8	144	108($\text{C}_5\text{H}_4\text{N}_2\text{O}^+$); 90($\text{C}_5\text{H}_2\text{N}_2^+$); 77($\text{C}_2\text{H}_3\text{O}_3^+$); 67($\text{C}_3\text{H}_3\text{N}_2^+$); 41(C_2NH_3^+); 28(CNH_2^+); 18(H_2O^+)		Yu et al.(2011) Kampf et al.(2012)
9	172	154($\text{C}_6\text{H}_6\text{N}_2\text{O}_3^+$); 136($\text{C}_6\text{H}_4\text{N}_2\text{O}_2^+$); 105($\text{C}_3\text{H}_3\text{O}_4^+$); 67($\text{C}_3\text{H}_3\text{N}_2^+$); 41(C_2NH_3^+); 29(CHO^+); 18(H_2O^+)		Yu et al.(2011) Kampf et al.(2012)
10	190	123($\text{C}_3\text{H}_7\text{O}_5^+$); 67($\text{C}_3\text{H}_3\text{N}_2^+$); 113($\text{C}_4\text{H}_5\text{N}_2\text{O}_2^+$); 77($\text{C}_2\text{H}_3\text{O}_3^+$); 41(C_2NH_3^+); 28(CH_2N^+); 18(H_2O^+)		Yu et al.(2011) Kampf et al.(2012)
11	192	163($\text{C}_7\text{H}_7\text{N}_4\text{O}^+$); 133($\text{C}_6\text{H}_5\text{N}_4^+$); 67($\text{C}_3\text{H}_3\text{N}_2^+$); 41(C_2NH_3^+)		Yu et al.(2011) Kampf et al.(2012)
12	202	166($\text{C}_7\text{H}_6\text{N}_2\text{O}_3^+$); 135($\text{C}_4\text{H}_7\text{O}_5^+$); 117($\text{C}_4\text{H}_5\text{O}_4^+$); 67($\text{C}_3\text{H}_3\text{N}_2^+$); 41(C_2NH_3^+)		Yu et al.(2011) Kampf et al.(2012)

2,2'-biimidazole (BI) (13) after dehydration, and BI further hydration with (2) to generate mono glyoxal substituted 2,2'-biimidazole (GBI) (14) (Kampf et al. 2012).

As shown in Fig. 5, the mass spectra of class 13 to class 17 has many mass spectra peaks among m/z 0–600, and the 17th class with maximum m/z up to 600, indicating that HMW products are present in the aged benzene SOA particles in the presence of high concentration of $(\text{NH}_4)_2\text{SO}_4$ seed aerosol. As mentioned before, the retention of water on the $(\text{NH}_4)_2\text{SO}_4$ particles creating ammonium ion, which can promote the formation of HMW products through multiphase reactions such as hydration and polymerization of aldehydes form from OH-initiated

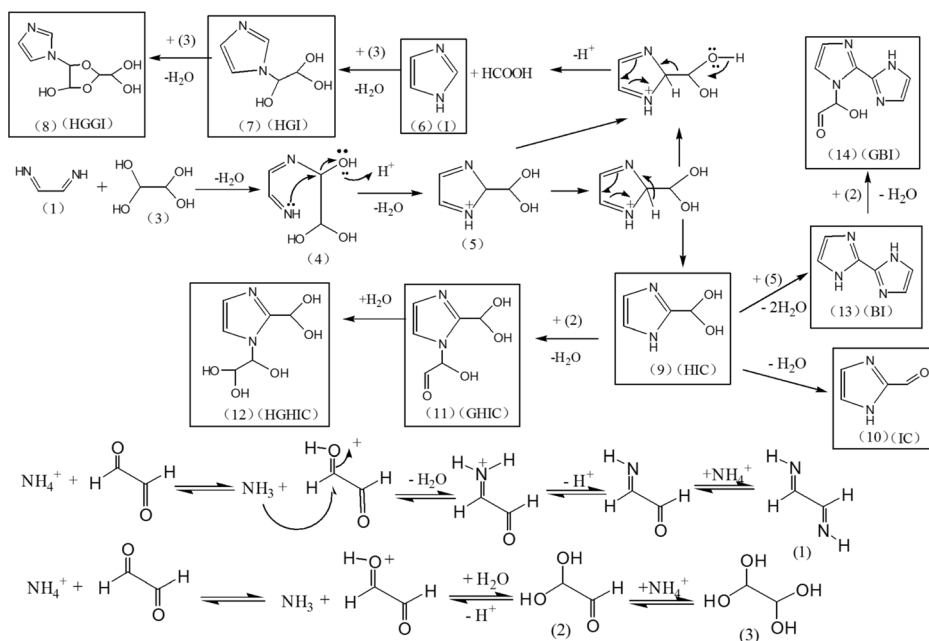


Fig. 6 Proposed reaction mechanisms for the imidazole compounds formation in the aging of benzene SOA in the presence of high concentration of $(\text{NH}_4)_2\text{SO}_4$ seed aerosol

oxidation of benzene (Jang et al. 2002; Gross et al. 2006). As mentioned above, ammonium ion acts as catalyst in the classical acid-catalyzed mechanism for the hydration of aldehydes. Accordingly, in the pathway of this mechanism, aldehyde is protonated by the ammonium ion, and the protonated aldehyde can undergo nucleophilic attack by H_2O followed by loss of H^+ ion, giving the corresponding diol product, which can be hydrolyzed to form tetrol product (Nozière et al. 2009). As shown in Fig. 7, the generated glyoxal could condense on the existing $(\text{NH}_4)_2\text{SO}_4$ seed aerosol, and be hydrated to form diol product (i), and tetrol product (ii). Two diol products (i) can react through nucleophilic attack of an OH group on the reactive carbonyl of the neighboring molecule to produce five-membered 1,3-dioxolane rings product (iii), which can then react with a third diol product (i), forming the stable glyoxal trimer (which contains two dioxolane rings) (iv) (Kua et al. 2008). While (iv) has been observed in laboratory experiment (Avzianova and Brooks 2013). The formed glyoxal trimer (iv) can continue to react with diol products (i) to generate HMW products. Similarly, diol products (i) may react with tetrol product (ii) to form (v) and (vi) after dehydration and cyclization. (vi) can continue to react with (i) to generate HMW products. Similar to glyoxal, 6-oxo-2,4-hexadienal and 2,3-epoxy-6-oxo-4-hexenal could be hydrated to form diol product (vii) and (viii), respectively. The cross-reacts of (vii) and (viii) with (v) to produce (ix) and (x), respectively (Kalberer et al. 2004). (ix) and (x) can continue to react with diol product (i) to generate various HMW products as outlined in Fig. 7.

3.3 Comparison with previous $(\text{NH}_4)_2\text{SO}_4$ seed aerosol studies

Previous dry $(\text{NH}_4)_2\text{SO}_4$ seed aerosol chamber studies were focused on the effect on aromatic SOA formation. No enhancement in SOA formation due to the presence of low concentration of dry $(\text{NH}_4)_2\text{SO}_4$ seed aerosol was observed in experiments of Cocker et al. (2001). However,

conditions. Also, high $(\text{NH}_4)_2\text{SO}_4$ concentration provides more reactive sites for multiphase reactions. Thus, the $(\text{NH}_4)_2\text{SO}_4$ seed aerosol induces the acid-catalyzed multiphase reactions, such as hydration and polymerization of aldehydes form from OH-initiated oxidation of benzene, and facilitates formation of imidazole compounds and HMW products as mentioned above. Compared to the experiments of Lu et al. (2009), our work extended the photooxidation time to 24 h, and the chemical compositions of the aged benzene SOA obtained by ALTOFMS coupled with FCM clustering algorithm further strengthen the suggestion that the effect of dry $(\text{NH}_4)_2\text{SO}_4$ on aromatic SOA is found to be positively correlated with the concentration of $(\text{NH}_4)_2\text{SO}_4$, the aromatic SOA enhancement is achieved by multiphase reactions induced and catalyzed by the ammonium ion of dry $(\text{NH}_4)_2\text{SO}_4$ seed aerosol.

4 Conclusion and atmospheric implications

$(\text{NH}_4)_2\text{SO}_4$ is the major inorganic aerosol species in urban atmosphere, which can play an important role in aromatic SOA formation and aging. Our experimental results suggest that the low concentration of dry $(\text{NH}_4)_2\text{SO}_4$ acts just as the nucleation or condensation center of the SOA, and do not affect the chemical composition of the aged benzene SOA. However, the high concentration (about $100 \mu\text{g m}^{-3}$) of dry $(\text{NH}_4)_2\text{SO}_4$ can promote the formation of imidazole compounds and high-molecular-weight products in the aged benzene SOA. Although the concentrations of benzene and NO_x in our smog experiments are several orders of magnitude higher than that in the ambient atmosphere, the effect of high concentrations of dry $(\text{NH}_4)_2\text{SO}_4$ seed aerosol is still expected to be prevalent in the atmosphere since the atmospheric organic aerosol mass loading is low, under which condition the incidence of dry $(\text{NH}_4)_2\text{SO}_4$ effect could be high. Studies (Yu et al. 2011; Kampf et al. 2012; Nakayama et al. 2013) have shown that imidazole compounds and high-molecular-weight products can absorb solar radiation of ultraviolet-visible effectively, resulting in the decreasing the visibility of air. The optical properties of the aged aromatic SOA should be addressed in further experimental investigations.

Acknowledgments The authors thank Mr. Michael Nusbaum from Department of English, Xiamen University, Tan Kah Kee College for help with the English language. This work is supported by the National Natural Science Foundation of China (No. 41575118, 41305109, 21502086, 41575126), the Outstanding Youth Science Foundation of Fujian Province of China (No. 2015J06009) and the Natural Science Foundation of Fujian Province of China (No.2015 J05028). Also, the authors express our gratitude to the referees for their valuable comments.

References

- Andreae M.O.: A new look at aging aerosols. *Science*. **326**, 1493–1494 (2009)
- Atkinson R., Carter W.P.L., Winer A.M.: An experimental protocol for the determination of OH radical rate constants with organics using methyl nitrite photolysis as an OH radical source. *J. Air Pollut. Control Assess.* **31**, 1090–1092 (1981)
- Avzianova E., Brooks S.D.: Raman spectroscopy of glyoxal oligomers in aqueous solutions. *Spectrochim. Acta A Mol. Biomol. Spectrosc.* **101**, 40–48 (2013)
- Baltensperger U.: Aerosols in clearer focus. *Science*. **329**, 1468–1470 (2010)
- Bezdek J.C.: Pattern recognition with fuzzy objective function algorithms, pp. 43–93. Plenum Press, New York (1981)
- Borrásá E., Tortajada-Genarob L.A.: Secondary organic aerosol formation from the photo-oxidation of benzene. *Atmos. Environ.* **47**, 154–163 (2012)

- Bowman F.M., Odum J.R., Seinfeld J.H., Pandis S.N.: Mathematical model for gas–particle partitioning of secondary organic aerosols. *Atmos. Environ.* **31**, 3921–3931 (1997)
- Cao G., Jang M.: An SOA model for toluene oxidation in the presence of inorganic aerosols. *Environ. Sci. Technol.* **44**, 727–733 (2010)
- Chhabra P.S., Flagan R.C., Seinfeld J.H.: Elemental analysis of chamber organic aerosol using an aerodyne high-resolution aerosol mass spectrometer. *Atmos. Chem. Phys.* **10**, 4111–4131 (2010)
- Cocker D.R., Mader B.T., Kalberer M., Flagan R.C., Seinfeld J.H.: The effect of water on gas-particle partitioning of secondary organic aerosol: II. m-Xylene and 1,3,5-trimethylbenzene photooxidation systems. *Atmos. Environ.* **35**, 6073–6085 (2001)
- Gross D.S., Gälli M.E., Kalberer M., Prevot A.S.H., Dommen J., Alfarra M.R., Duplissy J., Gaeggeler K., Gascho A., Metzger A., Baltensperger U.: Real-time measurement of oligomeric species in secondary organic aerosol with the aerosol time-of-flight mass spectrometer. *Anal. Chem.* **78**, 2130–2137 (2006)
- He K.B., Yang F.M., Ma Y.L., Zhang Q., Yao X.H., Chan C.K., Cadle S., Chan T., Mulawa P.: The characteristics of PM_{2.5} in Beijing, China. *Atmos. Environ.* **35**, 4959–4970 (2001)
- Huang M.Q., Zhang W.J., Hao L.Q., Wang Z.Y., Zhao W.W., Gu X.J., Guo X.Y., Liu X.Y., Long B., Fang L.: Laser desorption/ionization mass spectrometric study of secondary organic aerosol formed from the photooxidation of aromatics. *J. Atmos. Chem.* **58**, 237–252 (2007)
- Huang M.Q., Hao L.Q., Gu X.J., Hu C.J., Zhao W.X., Wang Z.Y., Fang L., Zhang W.J.: Effects of inorganic seed aerosols on the growth and chemical composition of secondary organic aerosol formed from OH-initiated oxidation of toluene. *J. Atmos. Chem.* **70**, 151–164 (2013a)
- Huang M.Q., Hao L.Q., Guo X.Y., Hu C.J., Gu X.J., Zhao W.X., Wang Z.Y., Fang L., Zhang W.J.: Characterization of secondary organic aerosol particles using aerosol laser time-of-flight mass spectrometer coupled with FCM clustering algorithm. *Atmos. Environ.* **64**, 85–94 (2013b)
- Huang M.Q., Lin Y.H., Huang X.Y., Liu X.Q., Hu C.J., Gu X.J., Zhao W.X., Fang L., Zhang W.J.: Chemical analysis of aged benzene secondary organic aerosol using aerosol laser time-of-flight mass spectrometer. *J. Atmos. Chem.* **71**, 213–224 (2014)
- Huang M.Q., Lin Y.H., Huang X.Y., Liu X.Q., Guo X.Y., Hu C.J., Zhao W.X., Gu X.J., Fang L., Zhang W.J.: Experimental study of particulate products for aging of 1,3,5-trimethylbenzene secondary organic aerosol. *Atmos. Pollut. Res.* **6**, 209–219 (2015)
- Jang M., Czoschke N.M., Lee S., Kamens R.M.: Heterogeneous atmospheric aerosol production by acid-catalyzed particle-phase reactions. *Science*. **298**, 814–817 (2002)
- Kalberer M., Paulsen D., Sax M., Steinbacher M., Dommen J., Prevot A.S.H., Fisseha R., Weingartner E., Frankevich V., Zenobi R., Baltensperger U.: Identification of polymers as major components of atmospheric organic aerosols. *Science*. **303**, 1659–1662 (2004)
- Kampf C.J., Jakob R., Hoffmann T.: Identification and characterization of aging products in the glyoxal/ammonium sulfate system - implications for light-absorbing material in atmospheric aerosols. *Atmos. Chem. Phys.* **12**, 6323–6333 (2012)
- Kua J., Hanley S.W., De Haan D.O.: Thermodynamics and kinetics of glyoxal dimer formation: a computational study. *J. Phys. Chem. A*. **112**, 66–72 (2008)
- Lee H.J., Aiona P.K., Laskin A., Laskin J., Nizkorodov S.A.: Effect of solar radiation on the optical properties and molecular composition of laboratory proxies of atmospheric brown carbon. *Environ. Sci. Technol.* **48**, 10217–10226 (2014)
- Loza C.L., Chhabra P.S., Yee L.D., Craven J.S., Flagan R.C., Seinfeld J.H.: Chemical aging of m-xylene secondary organic aerosol: laboratory chamber study. *Atmos. Chem. Phys.* **12**, 151–167 (2012)
- Lu Z.F., Hao J.M., Takekawa H., Hu L.H., Li J.H.: Effect of high concentrations of inorganic seed aerosols on secondary organic aerosol formation in the m-xylene/NO_x photooxidation system. *Atmos. Environ.* **43**, 897–904 (2009)
- Martín-Reviejo M., Wirtz K.: Is benzene a precursor for secondary organic aerosol? *Environ. Sci. Technol.* **39**, 1045–1054 (2005)
- Meyer N.K., Duplissy J., Gysel M., Metzger A., Dommen J., Weingartner E., Alfarra M.R., Fletcher C., Good N., McFiggans G., Jonsson A.M., Hallquist M., Baltensperger U., Ristovski Z.D.: Analysis of the hygroscopic and volatile properties of ammonium sulphate seeded and un-seeded SOA particles. *Atmos. Chem. Phys.* **9**, 721–732 (2008)
- Nakayama T., Sato K., Matsumi Y., Imamura T., Yamazaki A., Uchiyama A.: Wavelength and NO_x dependent complex refractive index of SOAs generated from the photooxidation of toluene. *Atmos. Chem. Phys.* **13**, 531–545 (2013)
- Ng N.L., Canagaratna M.R., Jimenez J.L., Chhabra P.S., Seinfeld J.H., Worsnop D.R.: Changes in organic aerosol composition with aging inferred from aerosol mass spectra. *Atmos. Chem. Phys.* **11**, 6465–6474 (2011)
- Nozière B., Dziedzic P., Córdova A.: Products and kinetics of the liquid-phase reaction of glyoxal catalyzed by ammonium ions (NH₄⁺). *J. Phys. Chem. A*. **113**, 231–237 (2009)

- Pillar E.A., Camm R.C., Guzman M.I.: Catechol oxidation by ozone and hydroxyl radicals at the air-water interface. *Environ. Sci. Technol.* **48**, 14352–14360 (2014)
- Prinn R.G., Huang J., Weiss R.F., Cunnold D.M., Fraser P.J., Simmonds P.G., McCulloch A., Harth C., Salameh P., O'Doherty S., Wang R.H.J., Porter L., Miller B.R.: Evidence for substantial variations of atmospheric hydroxyl radicals in the past two decades. *Science*. **292**, 1882–1888 (2001)
- Qi L., Nakao S., Malloy Q., Warren B., Cocker D.R.: Can secondary organic aerosol formed in an atmospheric simulation chamber continuously age? *Atmos. Environ.* **44**, 2990–2996 (2010)
- Rincón A.G., Guzmán M.I., Hoffmann M.R., Colussi A.J.: Optical absorptivity versus molecular composition of model organic aerosol matter. *J. Phys. Chem. A*. **113**, 10512–10520 (2009)
- Rincón A.G., Guzmán M.I., Hoffmann M.R., Colussi A.J.: Thermochromism of model organic aerosol matter. *J. Phys. Chem. Lett.* **1**, 368–373 (2010)
- Robinson A.L., Donahue N.M., Shrivastava M.K., Weitkamp E.A., Sage A.M., Grieshop A.P., Lane T.E., Pierce J.R., Pandis S.N.: Rethinking organic aerosols: semivolatile emissions and photochemical aging. *Science*. **315**, 1259–1262 (2007)
- Robinson C.B., Schill G.P., Zarzana K.J., Tolbert M.A.: Impact of organic coating on optical growth of ammonium sulfate particles. *Environ. Sci. Technol.* **47**, 13339–13346 (2013)
- Rudich Y., Donahue N.M., Mentel T.F.: Aging of organic aerosol: bridging the gap between laboratory and field studies. *Annu. Rev. Phys. Chem.* **58**, 321–352 (2007)
- Sareen N., Moussa S.G., McNeill V.F.: Photochemical aging of light-absorbing secondary organic aerosol material. *J. Phys. Chem. A*. **117**, 2987–2996 (2013)
- Sato K., Takami A., Kato Y., Seta T., Fujitani Y., Hikida T., Shimono A., Imamura T.: AMS and LC/MS analyses of SOA from the photooxidation of benzene and 1,3,5-trimethyl benzene in the presence of NO_x: effects of chemical structure on SOA aging. *Atmos. Chem. Phys.* **12**, 4667–4682 (2012)
- Schreier S.F., Peters E., Richter A., Lampel J., Wittrock F., Burrows J.P.: Ship-based MAX-DOAS measurements of tropospheric NO₂ and SO₂ in the South China and Sulu Sea. *Atmos. Environ.* **102**, 331–343 (2015)
- Singh A., Dey S.: Influence of aerosol composition on visibility in megacity Delhi. *Atmos. Environ.* **62**, 367–373 (2012)
- Sorooshian, A., Csavina, J., Shingler, T., Dey, S., Brechtel, F. J., Saez, A. E., Betterton, E. A.: Hygroscopic and chemical properties of aerosols collected near a copper smelter: implications for public and environmental health. *Environ. Sci. Technol.* **46**, 9473–9480 (2012)
- Tong D.L., Xu R.K.: Effects of urea and (NH₄)₂SO₄ on nitrification and acidification of ultisols from Southern China. *J. Environ. Sci.* **24**, 682–689 (2012)
- Topinka J., Rossner P., Milcova A., Schmuzerova J., Svecova V., Sram R.J.: DNA adducts and oxidative DNA damage induced by organic extracts from PM_{2.5} in an acellular assay. *Toxicol. Lett.* **202**, 186–192 (2011)
- Tritscher T., Dommen J., DeCarlo P.F., Gysel M., Barnet P.B., Praplan A.P., Weingartner E., Prévôt H.A.S., Riipinen I., Donahue N.M., Baltensperger U.: Volatility and hygroscopicity of aging secondary organic aerosol in a smog chamber. *Atmos. Chem. Phys.* **11**, 11477–11496 (2011)
- Updyke K.M., Nguyen T.B., Nizkorodov S.A.: Formation of brown carbon via reactions of ammonia with secondary organic aerosols from biogenic and anthropogenic precursors. *Atmos. Environ.* **63**, 22–31 (2012)
- Wang Y., Zhuang G., Sun Y., An Z.: The variation of characteristics and formation mechanisms of aerosols in dust, haze, and clear days in Beijing. *Atmos. Environ.* **40**, 6579–6591 (2006)
- Wang S.X., Xing J., Jang C., Zhu Y., Fu J.S., Hao J.M.: Impact assessment of ammonia emissions on inorganic aerosols in East China using response surface modeling technique. *Environ. Sci. Technol.* **45**, 9293–9300 (2011)
- Wang L.M., Wu R.R., Xu C.: Atmospheric oxidation mechanism of benzene. Fates of alkoxy radical intermediates and revised mechanism. *J. Phys. Chem. A*. **117**, 14163–14168 (2013)
- Yu G., Bayer A.R., Galloway M.M., Korshavn K.J., Fry C.G., Keutsch F.N.: Glyoxal in aqueous ammonium sulfate solutions: products, kinetics and hydration effects. *Environ. Sci. Technol.* **45**, 6336–6342 (2011)